



## OPEN Unraveling the mechanisms of irAEs in endometrial cancer immunotherapy: insights from FAERS and scRNA-seq data

Lu Zhang<sup>1,2,3</sup>, Mengjie Yang<sup>1,2,3</sup>, Yiqian Zhang<sup>1,2</sup>, Jianfa Lan<sup>1</sup>✉ & Qionghua Chen<sup>1,2</sup>✉

Endometrial cancer (EC) is one of the most common malignancies in women. In recent years, immunotherapy has gradually become a significant treatment option. However, the mechanisms underlying immune checkpoint inhibitor (ICI)-related Adverse Events (AEs) remain poorly understood, posing significant challenges for optimizing clinical treatment strategies. This study aims to integrate the FAERS database and single-cell transcriptomic data to investigate potential mechanisms underlying PD-1 inhibitor-related AEs in EC immunotherapy, with a focus on exploring the PD-1-associated cell communication network and its potential compensatory activation pathways. Data related to AEs were extracted from the FAERS database. Disproportionality analyses, including Reporting Odds Ratio (ROR), Proportional Reporting Ratio (PRR), Bayesian Confidence Propagation Neural Network (BCPNN), and Multi-item Gamma Poisson Shrinker (MGPS), were used to quantify signals of immune-related AEs (irAEs) associated with ICIs. We compared the occurrence timing and characteristics of AEs across different drugs. Subsequently, scRNA-seq was performed to analyze the tumor microenvironment of EC, focusing on PD-1-high expressing cell populations. Cell Communication was analyzed and key receptor-ligand pairs were identified. From Q1 2004 to Q3 2024, 21,838,627 drug-related reports were retrieved from FAERS, including 2,202 related to ICIs. ICI-associated irAEs involved 26 organ systems, with general disorders, gastrointestinal disorders, and injury/poisoning as the top System Organ Class (SOC). Fatigue, product use issues, and diarrhea were the most reported Preferred Terms (PTs). PD-1 inhibitors were associated with faster onset of AEs compared to PD-L1 inhibitors and Weibull modeling indicated an early failure-type AE pattern for both treatments. Single-cell analysis further demonstrated that PD-1 was highly expressed in CD8<sup>+</sup> cytotoxic T cells and Tfh cells, which communicated with other cells within the tumor microenvironment through key receptor-ligand pairs such as CXCL12-CXCR4 and CXCL16-CXCR6. These findings suggested that PD-1 inhibitors may induce AEs through compensatory activation of the CXCR4 and CXCR6 pathways. This study suggested that PD-1 inhibitors may contribute to irAEs in EC, potentially through compensatory activation of the CXCR4 and CXCR6 pathways. By integrating FAERS and scRNA-seq data, key receptor-ligand interactions were identified, providing preliminary insights that could inform future efforts to optimize immunotherapy efficacy and mitigate AEs. However, further validation through clinical studies and mechanistic research is needed to confirm these findings.

**Keywords** Endometrial cancer, Immunotherapy, PD-1 inhibitors, Adverse events, Single-cell analysis, FAERS database

Endometrial Cancer (EC) is one of the most common malignancies of the female reproductive system, with its incidence steadily rising globally, particularly in regions with a higher prevalence of obesity and metabolic syndrome<sup>1</sup>. Traditional treatments for EC include surgery, radiation therapy, and chemotherapy; however,

<sup>1</sup>Laboratory of Research and Diagnosis of Gynecological Diseases of Xiamen City, Clinical Medical Research Center for Obstetrics and Gynecology Diseases of Fujian Province, Department of Obstetrics and Gynecology, the First Affiliated Hospital of Xiamen University, School of Medicine, Xiamen University, Xiamen, China. <sup>2</sup>National Institute for Data Science in Health and Medicine, Xiamen University, Xiamen, China. <sup>3</sup>Lu Zhang and Mengjie Yang: contributed equally. ✉email: yanjiushengdoctor@163.com; cqhua616@126.com

the efficacy of these therapies is limited in advanced or recurrent cases<sup>2</sup>. As a result, immune-based therapies targeting the tumor microenvironment have become a key focus of research and clinical application in recent years<sup>3</sup>. Immune Checkpoint Inhibitors (ICIs) restore T-cell anti-tumor activity by blocking inhibitory signaling pathways and have demonstrated significant efficacy in various solid tumors<sup>4</sup>. The main ICIs used in EC include PD-1 inhibitors (such as Pembrolizumab and Nivolumab), PD-L1 inhibitors (such as Atezolizumab and Durvalumab), and CTLA-4 inhibitors (such as Ipilimumab)<sup>5–9</sup>. While these drugs have shown promising results in certain patients, immune-related AEs (irAEs) have emerged as a major concern, negatively impacting patients' quality of life and the continuation of treatment. In particular, the mechanisms underlying Adverse Reactions (ADRs) associated with PD-1 inhibitors remain inadequately understood<sup>10,11</sup>.

The FDA Adverse Event Reporting System (FAERS) is a valuable database established by the U.S. Food and Drug Administration (FDA) for the identification and monitoring of drug-related AEs globally. A systematic analysis of FAERS data provided valuable insights into potential risks and patterns of AEs<sup>12–14</sup>. However, relying solely on FAERS data does not offer sufficient detail to uncover the cellular and molecular mechanisms behind these AEs<sup>15</sup>.

single-cell RNA sequencing (scRNA-seq) has recently emerged as a powerful tool for analyzing complex tissue microenvironments<sup>16–18</sup>. It enables the profiling of cell composition and state at single-cell resolution within tumors and their immune microenvironment, thereby uncovering potential cell-to-cell communication pathways<sup>17</sup>. This technique provides valuable insights for exploring the mechanisms of action of ICIs. By integrating the macro data from FAERS with the micro mechanisms revealed by single-cell analysis, this study aims to establish a connection between clinical observations and molecular mechanisms, making it possible to provide new avenues for understanding and managing AEs.

In this study, we analyzed the characteristics of immune-related AEs (irAEs) in EC patients using FAERS data. We further utilized scRNA-seq data to explore the cell communication network. This integrative approach revealed key receptor-ligand interactions, including the potential compensatory activation of CXCL12-CXCR4 and CXCL16-CXCR6 pathways, which may be associated with the occurrence of AEs. These findings contribute to a better understanding of the mechanisms underlying ICI-related side effects and may inform future research aimed at optimizing treatment strategies and mitigating ADRs.

## Methods

### Data source and study design

This study utilized the FAERS database, a publicly accessible spontaneous reporting system that provides data on drug-related AEs worldwide. FAERS data are available through the FDA website (<https://fis.fda.gov/extensions/FPD-QDE-FAERS/FPD-QDE-FAERS.html>) and are updated regularly. The study period was selected from the first quarter of 2004 to the third quarter of 2024 to ensure a sufficiently long time span for data analysis. Specific details on the data fields can be found in Fig. 1.

### Selection of drugs and disease

The study focused on AEs related to ICIs used in EC, including the following drugs: Nivolumab, Pembrolizumab, Atezolizumab, Durvalumab, Avelumab, Ipilimumab, Tislelizumab, Dostarlimab, Camrelizumab, and Sintilimab (see Table S1)<sup>19</sup>. These drugs were identified using the “DRUGNAME” and “PROD\_AI” fields in the FAERS

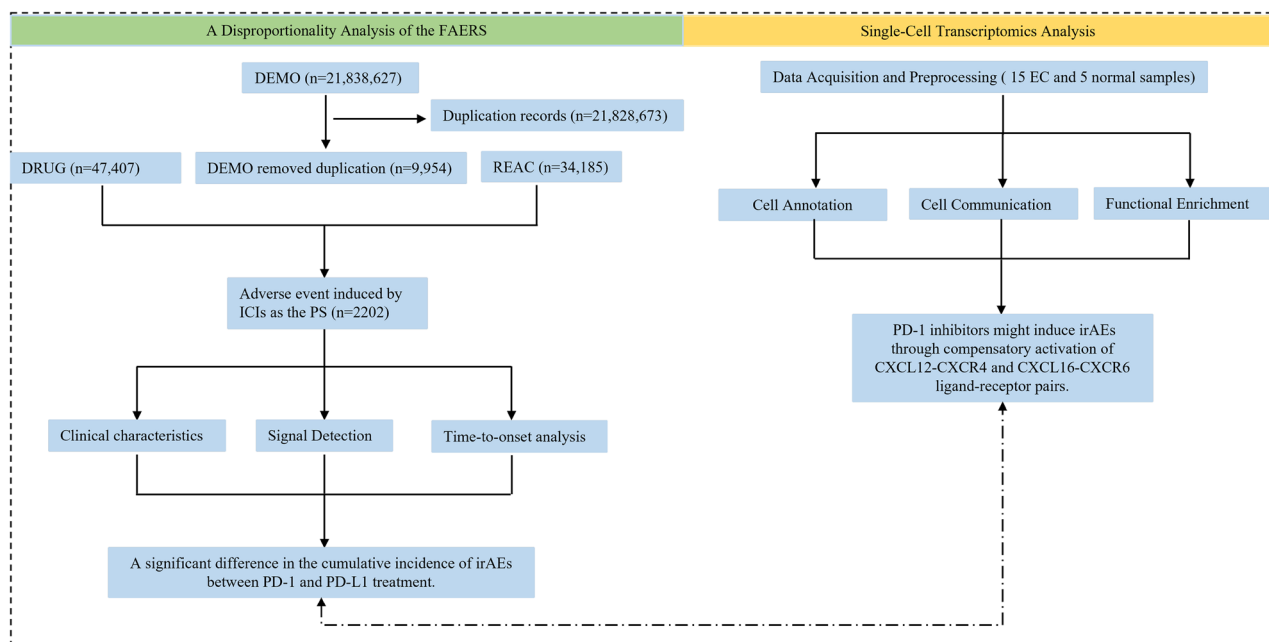


**Fig. 1.** Illustrated the workflow of FAERS and scRNA-seq analysis.

database, covering all variations of both generic and brand names. EC was selected as the disease of interest based on the “INDICATION” field in the case reports.

### Definition and classification of AEs

To identify irAEs associated with ICIs, the 27<sup>th</sup> version of the Medical Dictionary for Regulatory Activities (MedDRA) was used. “Immune system disorders” under the SOC category was selected for analysis, and further extraction of PTs was performed to classify and analyze the frequency of the AEs (see Table S2)<sup>20,21</sup>.

### Data cleaning and processing

Raw data were processed using R version 4.2.0. to eliminate the impact of duplicate or erroneous reports, the following data cleaning steps were applied: invalid reports explicitly marked as erroneous by the FDA were excluded, and deduplication was performed by retaining only the most recent version of each unique “CASEID.” Cases with identical age, event date, report country, adverse event, and drug information were treated as duplicates and merged or deleted<sup>22–24</sup>. Reports involving the specified ICIs as Primary Suspect (PS) drugs and related to “Endometrial Cancer” were extracted.

### Data mining algorithm

To identify potential safety signals, disproportionality analyses were conducted using the Proportional Reporting Ratio (PRR), Reporting Odds Ratio (ROR), the Bayesian confidence propagation neural network (BCPNN) and the Multi-item Gamma Poisson Shrinker (MGPS)<sup>25–27</sup>. The equations and criteria for the four algorithms were described as previously and shown in Table S3.

### Weibull distribution model

The model was defined by two parameters: the shape parameter ( $\alpha$ ) and the scale parameter ( $\beta$ ). The shape parameter ( $\alpha$ ) indicates the failure rate over time, where  $\alpha < 1$  suggests early failure (rapid onset of AEs),  $\alpha = 1$  indicates a constant failure rate (exponential distribution), and  $\alpha > 1$  implies a decreasing failure rate over time. The scale parameter ( $\beta$ ) determines the time scale at which events occur, with higher values indicating later onset.

### Statistical analysis

Descriptive statistics were used to summarize patient demographic data (e.g., age), reporter characteristics (e.g., occupation), and the time to event occurrence for reports where ICIs were identified as the PS drugs. Continuous variables, such as age and time to event, were reported as medians with interquartile ranges (IQRs), while categorical variables were presented as counts and percentages. Missing or incomplete data were categorized as “unknown” to ensure transparency in the analysis.

### Single-Cell RNA-Seq analysis

#### Data acquisition and preprocessing

We obtained publicly available scRNA-seq datasets from 15 EC samples and 5 normal endometrial tissues through established repositories<sup>17,28,29</sup>. Quality control steps included filtering based on UMI counts and mitochondrial gene expression levels to exclude low-quality cells in Table S4.

#### Clustering, dimensionality reduction, and annotation

Normalized expression data were used to identify highly variable genes, which were then subjected to principal component analysis (PCA) to reduce dimensionality<sup>30</sup>. The first 40 principal components were used to construct a two-dimensional representation of the data with uniform manifold approximation and projection (UMAP)<sup>31</sup>. Clustering was performed using the FindClusters function in Seurat, with a resolution parameter set to 0.3, which allowed for a clear separation of cell clusters while avoiding over-segmentation. Batch effects were corrected using the Harmony algorithm prior to clustering. Cell clusters were annotated based on canonical marker genes identified through differential expression analysis, which was conducted using the FindAllMarkers function in Seurat. Marker genes were defined as those with at least a 0.25 log-fold change and expression in  $\geq 25\%$  of cells in a cluster. Lymphocytes were selected for further analysis, and these cells were reclustered to explore subpopulation heterogeneity.

#### Cell communication and functional enrichment

This study investigated cell-cell communication between the lymphocyte clusters and other clusters in the tumor microenvironment and identified ligand-receptor pairs involved in signaling between cell populations<sup>32</sup>. Differentially expressed genes in specific subclusters were subjected to functional enrichment analysis using the ClusterProfiler package<sup>33</sup>, with gene set enrichment analysis (GSEA) performed for Kyoto Encyclopedia of Genes and Genomes (KEGG) pathways<sup>34</sup>.

## Results

### Descriptive analysis

From the first quarter of 2004 to the third quarter of 2024, after data cleaning, a total of 21,838,627 drug-related reports were obtained, of which 2,202 reports were related to the target drugs, as shown in Fig. 1. Our analysis revealed that since 2015, ICIs have been widely used for the treatment of EC. With the increasing use of these therapies, the number of AE reports has risen each year, with 2023 marking the highest reporting year (see Figure S1).

As shown in Table 1, regarding the weight distribution of reported patients, 14.9% of patients weighed between 50 kg and 100 kg, but more than half of the reports (79.6%) had missing weight information. In terms of serious outcome, except for the missing values and other serious events, hospitalization (17.5%) was the most frequently reported serious outcome, and death or life-threatening events were reported in 206 (9.4%) and 32 (1.5%) cases, respectively. In terms of reporter occupation, the largest proportion was consumers (53.0%), followed by physicians (29.6%) and health-professional (12.9%). The distribution of reports by country showed that the majority came from the United States (76.0%), followed by Japan (4.6%) and France (3.3%).

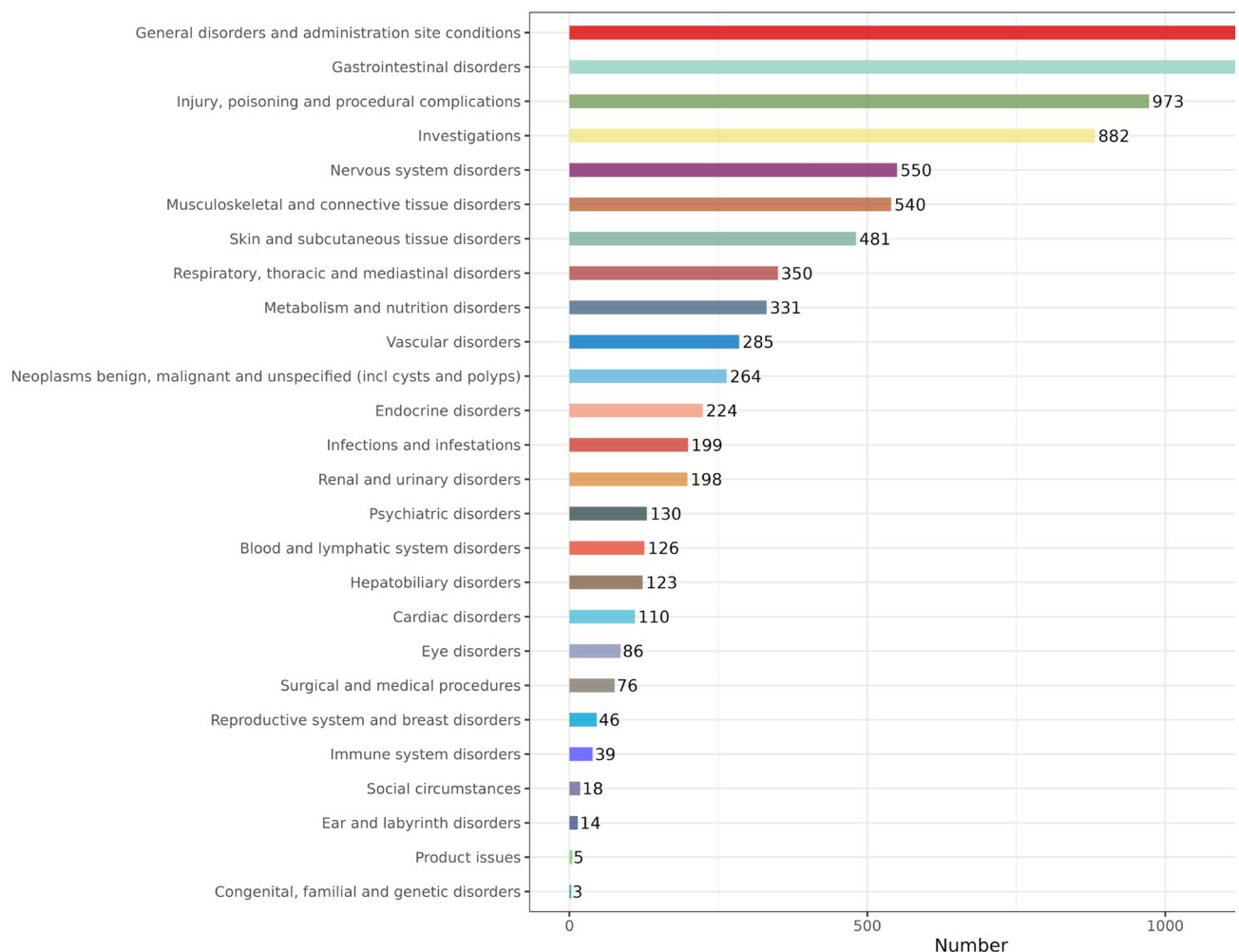
### Adverse event signal analysis

Figure 2 showed a total of 26 organ systems were involved in irAEs associated with ICIs. The top five categories of AEs (SOC level) were general disorders and administration site reactions, gastrointestinal disorders, injury, poisoning and procedural complications, Investigations and nervous system disorders. Figure 3 illustrated the signal strength of different SOC categories, with reports of injury, poisoning and procedural complications (ROR = 2.27), general disorders and administration site reactions (ROR = 1.1), skin and subcutaneous tissue disorders (ROR = 1.3), musculoskeletal and connective tissue disorders (ROR = 1.69), Investigations (ROR = 1.09), eye disorders (ROR = 1.37), surgical and medical procedures (ROR = 1.67) and social circumstances (ROR = 2.02) showing a ROR greater than 1, meeting the signal detection criteria. Detailed results are shown in Table 2.

As showed in Fig. 4, at the PT level, the most commonly reported symptoms were fatigue (3.86%), product use issue (3.71%), diarrhea (2.85%), inappropriate schedule of product administration (2.73%), malignant neoplasm progression (2.30%), hypertension (2.14%), and increased blood pressure (1.74%). The number of reporting PTs  $\geq 10$  were shown in Table 3. A total of 158 PTs and 21 corresponding SOC were detected after conforming to the four algorithms simultaneously with specific details available, and others were listed in Table S5. In this study, Stomatitis, abdominal discomfort, dysphagia, abdominal distension, glossodynia, haematochezia, feeding disorder, malignant neoplasm progression, drug-induced liver injury, thyroid disorder, immune-mediated

Characteristics	Case number, <i>n</i>	Case proportion, %
Number Of Events	2022	
Weight		
< 50 Kg	54	2.5
> 100 Kg	67	3.0
50 ~ 100 Kg	328	14.9
Missing	1753	79.6
Age		
$\leq 17$	13	0.6
$\geq 86$	7	0.3
18 ~ 64	412	18.7
65 ~ 85	668	30.3
Missing	1102	50.0
Reporter's type of occupation		
Consumer	1167	53.0
Health-professional	284	12.9
Physician	651	29.6
Other health-professional	37	1.7
Pharmacist	60	2.7
Missing	3	0.1
Serious Outcome		
Death	206	9.4
Disability	23	1.0
Hospitalization - Initial or Prolonged	386	17.5
Life-Threatening	32	1.5
Other Serious (Important Medical Event)	468	21.3
Missing	1087	49.4
Reporter's Country (Top Five)		
United States	1674	76.0
Japan	101	4.6
France	73	3.3
Korea, South	70	3.2
Canada	42	1.9

**Table 1.** Clinical characteristics of reports with immune checkpoint inhibitors from the FAERS database (January 2004 to September 2024).



**Fig. 2.** Signal number of AEs of ICIs at the System Organ Class (SOC) level in FAERS database.

hypothyroidism, fatigue, drug ineffective, adverse event, ill-defined disorder, feeling abnormal, gait disturbance, illness, adverse drug reaction, swelling, gait inability, treatment failure, rash, blister, rash pruritic, skin exfoliation, rash macular, skin lesion, arthralgia, myalgia, pain in extremity, muscle spasms, arthritis, myositis, musculoskeletal stiffness, limb discomfort, dysphonia, weight decreased, blood pressure abnormal, hepatic enzyme increased, blood thyroid stimulating hormone increased, thyroid function test abnormal, thyroid hormones increased, thyroid hormones decreased, liver function test increased, liver function test abnormal and lymphadenopathy were met the criteria for at least one of the four algorithms.

### Differences between PD-1 and PD-L1 immune responses

The onset times of ICIs-associated AEs were collected from the database. The results indicated that most of the onsets of AEs occurred within the first 1 ( $n = 2143$ , 7.92%), 2 ( $n = 1823$ , 6.74%), 3 ( $n = 2818$ , 10.42%), and 3 ~ 6 months ( $n = 4390$ , 16.23%) after initiation of ICIs. 41.52% of AEs occurred after 1 year, as shown in the analysis (Fig. 5A). By comparing adverse event occurrences between PD-1 and PD-L1 treatment groups, Fig. 5B demonstrated a significant difference in the cumulative incidence of irAEs (log-rank test,  $P < 0.0001$ ). Specifically, the median onset time for AEs in PD-L1-treated patients was significantly longer than in PD-1-treated patients, which may reflect differences in the timing or nature of immune-related adverse event development, although further mechanistic studies are required to clarify the underlying cause. Furthermore, the time-to-onset analysis using the Weibull distribution model revealed that AEs induced by both PD-1 and PD-L1 treatments exhibit an early failure-type pattern, as indicated by the shape parameters for PD-1 (0.71, 95% CI: 0.64–0.77) and PD-L1 (0.73, 95% CI: 0.60–0.87), both of which are less than 1 (Table 4). These findings suggested that the majority of AEs for both treatments occur relatively early after initiation of therapy.

### scRNA-seq data analysis

In previous study, we found that PD-1 inhibitors triggered AEs more rapidly than PD-L1 inhibitors, suggesting a potentially unique mechanism of action. To explore the biological basis of this phenomenon, we performed single-cell transcriptomic data analysis. Figure 6A presented the tumor microenvironment profile from the scRNA-seq data of EC (Figures S2A–S2B). Further analysis revealed lymphocytes accounted for a substantial proportion



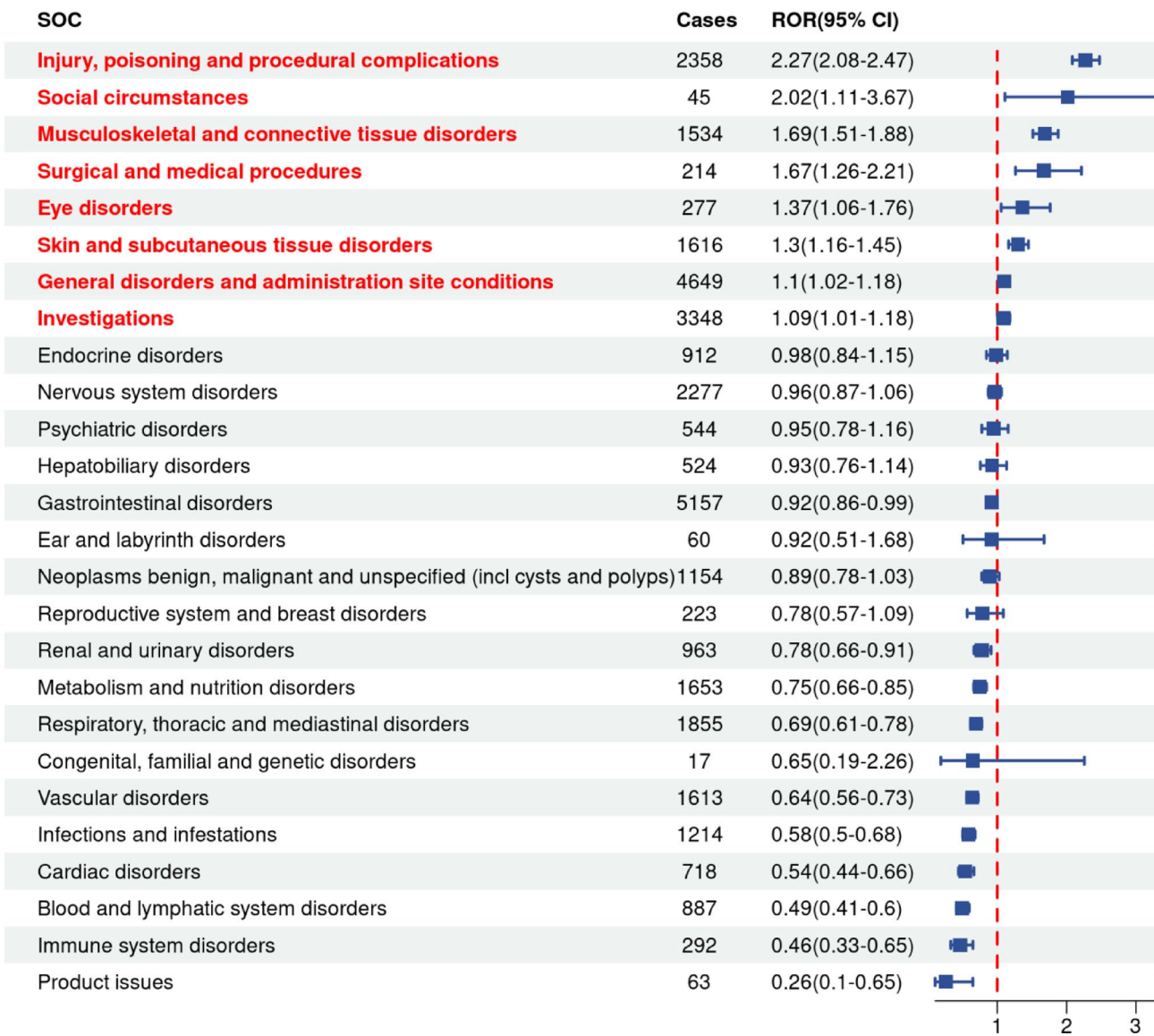


**Fig. 3.** Signal strength of AE of ICIs at the System Organ Class (SOC) level in FAERS database.

of cells within the tumor microenvironment (Fig. 6B), suggesting that lymphocytes played an important role. Based on this, we performed further sub-cluster analysis of lymphocyte cell populations, which were labeled as Naive T cells, CD8 + cytotoxic T cells, CD8 + Tissue-resident memory T cells (CD8\_Trm cells), regulatory T cells (Tregs), Follicula\_helper\_T cells (Tfh), T helper 17 cells (Th17\_cell), NKT cells, NK cells, B cells, Plasma cells and Mixed\_cell (Figs. 6C, Figures S2C-S2D). The results showed that CD8 + cytotoxic T cells represented a significant proportion of all sub-clusters (Fig. 6D). In pathway enrichment analysis, the lymphocyte sub-clusters were enriched in various signaling pathways. Specifically, CD8 + cytotoxic T cells were enriched in pathways such as cytokine–cytokine receptor interaction, chemokine signaling pathway, and viral protein interaction with cytokine and cytokine receptor. Meanwhile, Tfh cells showed enrichment in the cAMP signaling pathway, apelin signaling pathway, and purine metabolism (Fig. 6E). Further analysis showed that the PDCD1 gene was highly expressed in CD8 + cytotoxic T cells and Tfh cells. Meanwhile, PD-L1 was predominantly expressed in Tregs (Fig. 6F-G).

Cell communication analysis further revealed that CD8 + cytotoxic T cells and Tfh cells engaged in strong communication with other cells in the tumor microenvironment through key ligand-receptor pairs such as CXCL12-CXCR4 and CXCL16-CXCR6 (Fig. 7A, Figure S3-S4). In Fig. 7A, all plotted interactions are statistically significant ( $P < 0.01$ ), with color intensity indicating communication probability. These communication pathways were not observed in Tregs (Figure S5), suggesting that the pathways involving these ligand-receptor pairs might play a unique role under PD-1 inhibitor treatment, and this compensatory activation could potentially contribute to the rapid occurrence of irAEs. Further analysis of the CXCL pathways validated that CD8 + cytotoxic T cells and Tfh cells strongly communicated with stromal fibroblasts and endothelial cells (Fig. 7B and C). Given the

System Organ Class (SOC)	Cases (n)	ROR (95% two-sided CI)	PRR (χ2)	IC (IC025)	EBGM (EBGM05)
Gastrointestinal Disorders	5157	0.92 (0.86,0.99)	0.93 (5.39)	−0.08 (−1.74)	0.95 (0.88)
Metabolism and Nutrition Disorders	1653	0.75(0.66,0.85)	0.76 (21.64)	−0.31 (−1.98)	0.81 (0.71)
Neoplasms Benign, Malignant and Unspecified (Incl Cysts and Polyps)	1154	0.89 (0.78,1.03)	0.90(2.48)	−0.12 (−1.79)	0.92 (0.8)
Injury, Poisoning and Procedural Complications	2358	2.27 (2.08,2.47) *	2.12 (365.54) *	0.73 (−0.94)	1.66 (1.52)
Hepatobiliary Disorders	524	0.93 (0.76,1.14)	0.93 (0.54)	−0.08 (−1.75)	0.94 (0.77)
Nervous System Disorders	2277	0.96 (0.87,1.06)	0.96 (0.63)	−0.04 (−1.71)	0.97 (0.88)
Renal and Urinary Disorders	963	0.78(0.66,0.91)	0.78 (9.75)	−0.27 (−1.94)	0.83 (0.71)
Product Issues	63	0.266 (0.1,0.65)	0.26 (9.67)	−1.65 (−3.35)	0.32 (0.13)
Infections and Infestations	1214	0.58 (0.5,0.68)	0.59 (48.19)	−0.6 (−2.27)	0.66 (0.57)
Endocrine Disorders	912	0.98 (0.84,1.15)	0.98 (0.04)	−0.02 (−1.69)	0.99 (0.85)
Immune System Disorders	292	0.46 (0.33,0.65)	0.47 (20.83)	−0.9 (−2.57)	0.54 (0.38)
General Disorders and Administration Site Conditions	4649	1.10 (1.02,1.18) *	1.08 (6.69)	0.09 (−1.58)	1.06 (0.99)
Skin and Subcutaneous Tissue Disorders	1616	1.30 (1.16,1.45) *	1.28 (21.97)	0.26 (−1.41)	1.2 (1.07)
Musculoskeletal and Connective Tissue Disorders	1534	1.69 (1.51,1.88) *	1.64 (92.22)	0.5 (−1.16)	1.42 (1.27)
Respiratory, Thoracic and Mediastinal Disorders	1855	0.69 (0.61,0.78)	0.70 (37.55)	−0.4 (−2.06)	0.76 (0.67)
Investigations	3348	1.09 (1.01,1.18) *	1.08 (4.45)	0.08 (−1.58)	1.06 (0.98)
Reproductive System and Breast Disorders	223	0.78 (0.57,1.09)	0.79 (2.14)	−0.27 (−1.95)	0.83 (0.6)
Vascular Disorders	1613	0.64 (0.56,0.73)	0.65 (46.71)	−0.49 (−2.16)	0.71 (0.62)
Blood and Lymphatic System Disorders	887	0.49 (0.41,0.6)	0.50 (55.23)	−0.81 (−2.48)	0.57 (0.47)
Eye Disorders	277	1.37 (1.06,1.76) *	1.36 (5.75)	0.32 (−1.35)	1.25 (0.97)
Cardiac Disorders	718	0.54 (0.44,0.66)	0.55 (35.65)	−0.7 (−2.37)	0.62 (0.5)
Surgical and Medical Procedures	214	1.67 (1.26,2.21) *	1.67 (13.12)	0.52 (−1.16)	1.43 (1.08)
Psychiatric Disorders	544	0.95 (0.78,1.16)	0.95(0.27)	−0.06 (−1.73)	0.96 (0.79)
Ear and Labyrinth Disorders	60	0.92 (0.51,1.68)	0.92 (0.07)	−0.09 (−1.8)	0.94 (0.52)
Congenital, Familial and Genetic Disorders	17	0.65 (0.19,2.26)	0.65 (0.47)	−0.49 (−2.29)	0.71 (0.2)
Social Circumstances	45	2.02 (1.11,3.67) *	2.02 (5.54) *	0.69 (−1.03)	1.61 (0.89)

**Table 2.** Signal strength of AEs of immune checkpoint inhibitors at the system organ class (SOC) level in FAERS database. \*Indicates statistically significant signals in algorithm. ROR, reporting odds ratio; CI, confidence interval. PRR, proportional reporting ratio; χ2, chi-squared. IC, information component; IC025, the lower limit of the 95% CI of the IC. EBGM, empirical Bayesian geometric mean; EBGM05, the lower limit of 95% CI of EBGM.

significant proportion of these cells within the microenvironment (Fig. 6D), their intense interaction with other immune cells may contribute to the rapid occurrence of irAEs.

Discussion

This study identified irAEs associated with ICIs across 26 organ systems, with findings at both the SOC and PT levels. The top five SOC categories—general disorders and administration site reactions, gastrointestinal disorders, injury, poisoning and procedural complications, investigations, and nervous system disorders—highlighted the breadth of organ systems impacted. Notably, the ROR for categories such as injury, poisoning and procedural complications (ROR = 2.27) and musculoskeletal and connective tissue disorders (ROR = 1.69) exceeded 1, indicating strong signal detection. At the PT level, commonly reported AEs included fatigue (3.86%), product use issue (3.71%), and diarrhea (2.85%). These findings aligned with prior pharmacovigilance studies, underscoring that gastrointestinal and general systemic reactions remain prevalent irAEs across ICI treatments<sup>35</sup>. The detection of musculoskeletal disorders such as arthralgia, myalgia, and stiffness corroborated earlier studies linking T cell activation and inflammation mediated by ICIs to such outcomes. These musculoskeletal irAEs were reflective of heightened systemic immune activation. Similarly, thyroid and liver dysfunctions noted in our study were consistent with ICIs’ known impact on endocrine and hepatic pathways<sup>36</sup>. This finding highlighted the complexity of ICI-associated irAEs and underscored the importance of pharmacovigilance in identifying and characterizing these events.

This study systematically revealed the mechanisms underlying irAEs associated with ICIs in EC, integrating data from the FAERS database and single-cell transcriptomics data. Notably, it emphasized the differences in the occurrence of AEs between PD-1 and PD-L1 inhibitors. We found that PD-1 inhibitors induced AEs more rapidly than PD-L1 inhibitors, suggesting that PD-1 inhibitors may trigger more acute and swift immune reactions. Furthermore, through scRNA-seq data analysis, we further explored the roles of immune cells in the EC microenvironment, particularly the importance of CD8 + cytotoxic T cells and Tfh cells in immune-related ADRs. We proposed that PD-1 inhibitors might induce irAEs through compensatory activation of CXCL12-CXCR4 and CXCL16-CXCR6 ligand-receptor pairs, offering new insights into the mechanisms of irAEs in immunotherapy.

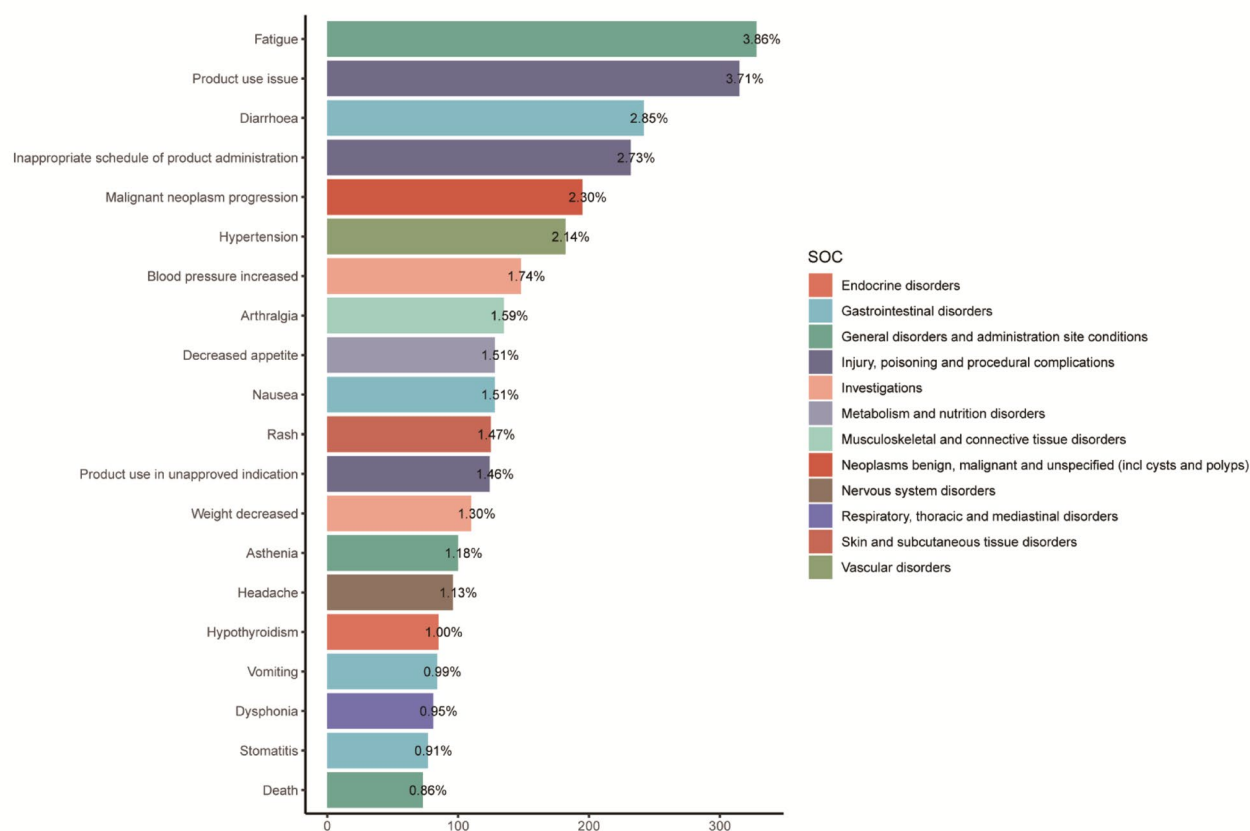


**Fig. 4.** Signal strength of AEs of ICIs at the PTs (PT) level in FAERS database.

The findings of this study were consistent with existing meta-analyses and clinical studies on ICIs. Several studies have examined the differences in the incidence and onset time of AEs between PD-1 and PD-L1 inhibitors<sup>37–39</sup>. Specifically, PD-1 inhibitors are generally considered to have a higher incidence and faster onset of AEs compared to PD-L1 inhibitors. According to some meta-analyses, there was a significant difference in the incidence of irAEs between PD-1 and PD-L1 inhibitors, particularly in skin, gastrointestinal, and endocrine system reactions. For example, Puzanov et al. in their review of ICIs noted that the irAEs induced by PD-1 inhibitors occur earlier and tend to be more severe, particularly in terms of rash, diarrhea, and endocrine disorders<sup>40</sup>. This suggested that PD-1 inhibitors may activate the immune system more intensely and broadly, leading to rapid progression of irAEs.

Consistent with these findings, our analysis of FAERS data revealed that the onset time of AEs associated with PD-1 inhibitors was shorter than that of PD-L1 inhibitors. This phenomenon suggested that PD-1 inhibitors may induce more severe immune reactions initially, leading to the rapid onset of AEs. Through detailed single-cell analysis, we further elucidated the behavior of immune cells in the tumor microenvironment, finding that PD-1 inhibitors may accelerate the occurrence of immune responses by modulating the activation of immune cell sub-clusters, including CD8 + cytotoxic T cells and Tfh cells. This finding aligned with previous studies indicating that PD-1 inhibitors strongly activate T cells, particularly in the context of anti-tumor immune responses, potentially triggering more immune reactions and increasing the likelihood and speed of AEs<sup>41</sup>. Several studies have demonstrated that the immune activation driving irAEs were linked to enhanced anti-tumor responses, suggesting a mechanistic overlap between the two phenomena<sup>42</sup>. Early-onset irAEs were often associated with better treatment responses, possibly reflecting early immune system engagement. Moderate to severe irAEs, despite requiring management, had been linked to greater therapeutic benefits. Mechanistically, severe irAEs may reflect strong activation of effector T cells, which played a pivotal role in anti-tumor immunity<sup>43</sup>.

Khoja et al. observed that AEs such as pneumonitis, hypothyroidism, and arthralgia are more frequently linked to anti-PD-1 therapies compared to anti-CTLA-4 therapies. Specifically, pembrolizumab was associated with an elevated risk of pneumonitis and arthralgia, while nivolumab exhibited a stronger correlation with hypothyroidism<sup>44</sup>. These findings had been hypothesized to stem from variations in the tumor microenvironment, differential expression of immune-related genes, and individual patient responses to ICIs<sup>45</sup>. However, the precise mechanisms remained under investigation. Building on this foundation, our research provided additional insights by examining the tumor microenvironment and gene expression profiles. Through scRNA-seq and immune-related pathway analysis, we further elucidated the potential molecular and cellular mechanisms underpinning these AEs.



System Organ Class (SOC)	Preferred terms (PTs)	Cases (n)	ROR (95% two-sided CI)	PRR ( $\chi^2$ )	IC (IC025)	EBGM (EBGM05)
Gastrointestinal disorders	Diarrhoea	242	1.14 (0.98,1.32)	1.14 (2.96)	0.14 (−1.53)	1.10 (0.95)
	Nausea	128	0.65 (0.53,0.79)	0.65 (19.85)	−0.49 (−2.15)	0.71 (0.59)
	Vomiting	84	0.58 (0.46,0.73)	0.58 (21.76)	−0.63 (−2.30)	0.65 (0.51)
	Stomatitis	77	1.60 (1.21,2.11) *	1.60 (11.27)	0.47 (−1.20)	1.39 (1.05)
	Constipation	63	0.89 (0.67,1.17)	0.89 (0.72)	−0.13 (−1.81)	0.91 (0.69)
	Abdominal Pain	60	0.66 (0.50,0.88)	0.67 (8.24)	−0.46 (−2.13)	0.73 (0.55)
	Colitis	45	1.39 (0.98,1.98)	1.39 (3.37)	0.34 (−1.34)	1.27 (0.89)
	Abdominal Pain Upper	32	1.02 (0.68,1.52)	1.02 (0.01)	0.02 (−1.67)	1.01 (0.68)
	Dry Mouth	29	1.20 (0.78,1.85)	1.20 (0.70)	0.19 (−1.50)	1.14 (0.74)
	Abdominal Discomfort	26	1.68 (1.04,2.71) *	1.67 (4.54)	0.52 (−1.18)	1.43 (0.89)
	Dysphagia	22	2.30 (1.32,4.00) *	2.29 (9.15) *	0.80 (−0.92)	1.74 (1.00)
	Oral Pain	22	1.21 (0.74,1.99)	1.21 (0.57)	0.20 (−1.50)	1.15 (0.70)
	Abdominal Distension	20	1.73 (1.00,3.00) *	1.73 (3.91)	0.55 (−1.16)	1.46 (0.84)
	Dyspepsia	19	1.55 (0.89,2.70)	1.55 (2.48)	0.45 (−1.26)	1.37 (0.78)
	Ascites	15	0.77 (0.44,1.36)	0.77 (0.83)	−0.29 (−1.99)	0.82 (0.46)
	Intestinal Perforation	14	0.64 (0.36,1.14)	0.64 (2.32)	−0.51 (−2.20)	0.70 (0.40)
	Intestinal Obstruction	13	0.89 (0.48,1.66)	0.89 (0.13)	−0.12 (−1.83)	0.92 (0.49)
	Glossodynia	13	2.07 (1.02,4.20) *	2.07 (4.27) *	0.71 (−1.03)	1.63 (0.81)
	Pancreatitis	12	0.53 (0.28,0.97)	0.53 (4.38)	−0.75 (−2.44)	0.60 (0.32)
	Large Intestine Perforation	10	1.01 (0.49,2.06)	1.01 (0.00)	0.01 (−1.72)	1.01 (0.49)
Metabolism and Nutrition Disorders	Haematochezia	10	2.33 (1.02,5.31) *	2.33 (4.28) *	0.81 (−0.96)	1.75 (0.77)
	Gastrointestinal Disorder	10	1.32 (0.63,2.76)	1.32 (0.53)	0.29 (−1.45)	1.22 (0.58)
	Decreased appetite	128	0.92 (0.76,1.13)	0.92 (0.62)	−0.09 (−1.76)	0.94 (0.77)
	Dehydration	51	0.51 (0.38,0.69)	0.52 (19.78)	−0.77 (−2.44)	0.59 (0.44)
	Hyponatraemia	16	0.47 (0.28,0.79)	0.47 (8.31)	−0.89 (−2.57)	0.54 (0.32)
	Diabetes mellitus	13	1.64 (0.83,3.22)	1.64 (2.10)	0.50 (−1.23)	1.41 (0.72)
	Feeding disorder	13	2.62 (1.25,5.52) *	2.62 (6.99) *	0.90 (−0.85)	1.87 (0.89)
	Type 1 diabetes mellitus	11	0.92 (0.47,1.82)	0.92 (0.05)	−0.09 (−1.80)	0.94 (0.48)
	Hypophagia	10	1.12 (0.54,2.32)	1.12 (0.09)	0.12 (−1.61)	1.09 (0.53)
	Hyperkalaemia	10	1.89 (0.86,4.17)	1.89 (2.58)	0.63 (−1.13)	1.55 (0.70)
Neoplasms Benign, Malignant and Unspecified (Incl Cysts and Polyps)	Malignant neoplasm progression	195	1.35 (1.14,1.60) *	1.34 (12.08)	0.31 (−1.36)	1.24 (1.04)
Injury, Poisoning and Procedural Complications	Product use issue	315	15.92 (12.11,20.93) *	15.37 (703.59) *	1.75 (0.08) *	3.36 (2.56) *
	Inappropriate schedule of product administration	232	20.01 (14.07,28.45) *	19.49 (551.04) *	1.80 (0.13)	3.48 (2.45) *
	Product use in unapproved indication	124	1.69 (1.36,2.11) *	1.68 (22.25)	0.52 (−1.15)	1.44 (1.15)
	Off label use	67	0.36 (0.28,0.46)	0.36 (67.77)	−1.21 (−2.88)	0.43 (0.33)
	Incorrect dose administered	52	12.17 (6.62,22.35) *	12.10 (106.08) *	1.69 (−0.02)	3.22 (1.75)
	Product dose omission issue	29	3.38 (1.99,5.74) *	3.37 (22.93) *	1.09 (−0.62)	2.12 (1.25)
	Intentional product use issue	27	2.27 (1.38,3.75) *	2.27 (10.96) *	0.79 (−0.92)	1.72 (1.05)
	Product prescribing issue	24	24.26 (7.30,80.59) *	24.20 (59.35) *	1.84 (0.09)	3.58 (1.08)
	Fall	14	0.74 (0.41,1.33)	0.74 (1.00)	−0.33 (−2.03)	0.79 (0.44)
Hepatobiliary disorders	Hepatitis	15	1.19 (0.66,2.17)	1.19 (0.34)	0.19 (−1.52)	1.14 (0.63)
	Liver disorder	12	1.13 (0.58,2.20)	1.13 (0.14)	0.13 (−1.59)	1.10 (0.57)
	Drug-induced liver injury	12	2.59 (1.20,5.61) *	2.59 (6.33) *	0.89 (−0.86)	1.86 (0.86)
Nervous system disorders	Headache	96	1.17 (0.92,1.48)	1.17 (1.66)	0.16 (−1.51)	1.12 (0.88)
	Neuropathy peripheral	40	1.26 (0.87,1.83)	1.26 (1.52)	0.24 (−1.44)	1.18 (0.82)
	Dizziness	32	0.73 (0.50,1.08)	0.73 (2.51)	−0.35 (−2.03)	0.79 (0.53)
	Somnolence	22	0.82 (0.51,1.32)	0.82 (0.67)	−0.22 (−1.91)	0.86 (0.54)
	Cerebrovascular accident	18	0.62 (0.38,1.04)	0.63 (3.35)	−0.54 (−2.22)	0.69 (0.42)
	Balance disorder	17	1.77 (0.97,3.23)	1.77 (3.62)	0.57 (−1.15)	1.49 (0.82)
	Memory impairment	15	1.62 (0.87,3.04)	1.62 (2.32)	0.49 (−1.23)	1.40 (0.75)
	Hypoaesthesia	14	1.37 (0.73,2.57)	1.37 (0.95)	0.32 (−1.40)	1.25 (0.67)
	Cerebral haemorrhage	12	1.30 (0.66,2.55)	1.30 (0.57)	0.27 (−1.45)	1.21 (0.61)
	Paraesthesia	12	0.98 (0.51,1.88)	0.98 (0.00)	−0.02 (−1.74)	0.99 (0.51)
	Posterior reversible encephalopathy syndrome	11	0.79 (0.41,1.54)	0.79 (0.48)	−0.26 (−1.97)	0.84 (0.43)
	Tremor	11	0.63 (0.33,1.20)	0.63 (2.01)	−0.53 (−2.24)	0.69 (0.36)
	Taste disorder	11	0.88 (0.45,1.71)	0.88 (0.15)	−0.15 (−1.86)	0.90 (0.46)
	Seizure	10	0.56 (0.28,1.10)	0.56 (2.92)	−0.67 (−2.37)	0.63 (0.32)
	Hypersomnia	10	1.59 (0.74,3.43)	1.59 (1.44)	0.47 (−1.27)	1.39 (0.65)
Renal and Urinary Disorders	Proteinuria	56	1.23 (0.90,1.68)	1.23 (1.69)	0.22 (−1.46)	1.16 (0.85)
	Acute kidney injury	25	0.71 (0.46,1.10)	0.71 (2.34)	−0.38 (−2.07)	0.77 (0.50)
	Renal impairment	17	0.29 (0.18,0.48)	0.30 (26.16)	−1.48 (−3.16)	0.36 (0.22)
	Renal failure	14	0.55 (0.31,0.97)	0.55 (4.38)	−0.69 (−2.38)	0.62 (0.35)
Infections and Infestations	Urinary tract infection	30	0.59 (0.40,0.87)	0.59 (7.23)	−0.61 (−2.29)	0.66 (0.44)
	Sepsis	22	0.76 (0.47,1.21)	0.76 (1.39)	−0.31 (−2.00)	0.80 (0.50)
	Pneumonia	16	0.71 (0.41,1.23)	0.71 (1.52)	−0.38 (−2.08)	0.77 (0.44)
	Covid-19	15	1.46 (0.79,2.71)	1.46 (1.49)	0.39 (−1.33)	1.31 (0.71)
Endocrine disorders	Hypothyroidism	85	0.82 (0.65,1.05)	0.82 (2.54)	−0.21 (−1.89)	0.86 (0.68)
	Thyroid disorder	46	3.10 (2.06,4.68) *	3.09 (32.28) *	1.02 (−0.67)	2.03 (1.35)
	Hyperthyroidism	29	1.37 (0.88,2.13)	1.37 (2.00)	0.33 (−1.36)	1.25 (0.81)
	Adrenal insufficiency	13	0.32 (0.18,0.57)	0.32 (16.81)	−1.37 (−3.05)	0.39 (0.22)
	Immune-mediated hypothyroidism	12	18.17 (4.07,81.21)	18.15 (27.79) *	1.79 (−0.04)	3.45 (0.77)
Immune system disorders	Hypersensitivity	10	0.37 (0.19,0.72)	0.37 (9.38)	−1.18 (−2.87)	0.44 (0.23)
Continued						

System Organ Class (SOC)	Preferred terms (PTs)	Cases (n)	ROR (95% two-sided CI)	PRR (χ2)	IC (IC025)	EBGM (EBGM05)
General Disorders and Administration Site Conditions	Fatigue	328	1.58 (1.38,1.81) *	1.55 (44.16)	0.45 (−1.22)	1.37 (1.19)
	Asthenia	100	0.94 (0.75,1.18)	0.94 (0.30)	−0.07 (−1.74)	0.95 (0.76)
	Death	73	1.05 (0.80,1.37)	1.05 (0.11)	0.05 (−1.63)	1.03 (0.79)
	Pyrexia	67	0.50 (0.38,0.65)	0.50 (28.63)	−0.80 (−2.47)	0.57 (0.44)
	Drug ineffective	66	1.87 (1.38,2.55) *	1.87 (16.48)	0.62 (−1.06)	1.54 (1.13)
	Pain	63	1.15 (0.86,1.54)	1.15 (0.88)	0.15 (−1.53)	1.11 (0.83)
	Malaise	49	0.48 (0.35,0.64)	0.48 (24.13)	−0.86 (−2.53)	0.55 (0.41)
	Adverse event	41	12.46 (6.24,24.88) *	12.40 (84.39) *	1.69 (−0.02)	3.24 (1.62)
	Ill-defined disorder	40	12.15 (6.07,24.31) *	12.10 (81.57) *	1.69 (−0.03)	3.22 (1.61)
	Feeling abnormal	34	1.98 (1.29,3.06) *	1.98 (9.96)	0.67 (−1.02)	1.59 (1.03)
	Peripheral swelling	31	1.40 (0.91,2.15)	1.40 (2.42)	0.35 (−1.34)	1.27 (0.83)
	Gait disturbance	24	1.65 (1.00,2.72) *	1.65 (3.98)	0.51 (−1.20)	1.42 (0.86)
	Illness	16	2.31 (1.20,4.42) *	2.30 (6.71) *	0.80 (−0.93)	1.74 (0.91)
	Chills	15	0.73 (0.42,1.29)	0.73 (1.19)	−0.35 (−2.05)	0.78 (0.45)
	Drug intolerance	15	0.59 (0.34,1.02)	0.59 (3.61)	−0.61 (−2.30)	0.66 (0.38)
	No adverse event	14	1.41 (0.75,2.66)	1.41 (1.15)	0.36 (−1.36)	1.28 (0.68)
	General physical health deterioration	14	0.80 (0.44,1.44)	0.80 (0.56)	−0.25 (−1.95)	0.84 (0.47)
	Oedema peripheral	14	0.90 (0.50,1.64)	0.90 (0.12)	−0.11 (−1.82)	0.92 (0.51)
	Adverse drug reaction	14	2.65 (1.29,5.43) *	2.65 (7.66) *	0.91 (−0.84)	1.88 (0.92)
	Mucosal inflammation	12	0.77 (0.41,1.46)	0.77 (0.64)	−0.29 (−2.00)	0.82 (0.43)
	Swelling	10	4.32 (1.65,11.37) *	4.32 (10.51) *	1.24 (−0.56)	2.37 (0.90)
	Gait inability	10	3.36 (1.37,8.28) *	3.36 (7.86) *	1.08 (−0.70)	2.12 (0.86)
	Drug interaction	10	1.16 (0.56,2.41)	1.16 (0.17)	0.16 (−1.57)	1.12 (0.54)
	Treatment failure	10	4.32 (1.65,11.37) *	4.32 (10.51) *	1.24 (−0.56)	2.37 (0.90)
	Feeling cold	10	1.78 (0.81,3.89)	1.78 (2.15)	0.58 (−1.18)	1.49 (0.68)
Skin and Subcutaneous Tissue Disorders	Rash	125	1.74 (1.39,2.17) *	1.73 (24.57)	0.55 (−1.12)	1.46 (1.17)
	Palmar-plantar erythrodysesthesia syndrome	47	0.95 (0.69,1.33)	0.95 (0.08)	−0.05 (−1.73)	0.97 (0.69)
	Pruritus	38	1.35 (0.92,1.99)	1.35 (2.42)	0.31 (−1.37)	1.24 (0.85)
	Blister	24	3.03 (1.72,5.34) *	3.02 (16.29) *	1.01 (−0.71)	2.01 (1.14)
	Rash pruritic	21	3.35 (1.80,6.23) *	3.34 (16.40) *	1.08 (−0.65)	2.11 (1.14)
	Urticaria	18	1.43 (0.82,2.51)	1.43 (1.60)	0.37 (−1.34)	1.29 (0.74)
	Skin exfoliation	17	2.24 (1.20,4.19) *	2.24 (6.68) *	0.77 (−0.95)	1.71 (0.91)
	Dry skin	11	1.45 (0.71,2.97)	1.45 (1.03)	0.38 (−1.36)	1.30 (0.63)
	Erythema	11	0.29 (0.16,0.55)	0.29 (17.01)	−1.49 (−3.17)	0.36 (0.19)
	Rash macular	10	4.32 (1.65,11.37) *	4.32 (10.51) *	1.24 (−0.56)	2.37 (0.90)
	Skin lesion	10	6.06 (2.07,17.72) *	6.05 (14.05) *	1.42 (−0.39)	2.68 (0.92)
Musculoskeletal and Connective Tissue Disorders	Arthralgia	135	2.09 (1.68,2.61) *	2.07 (44.91) *	0.71 (−0.96)	1.64 (1.31)
	Myalgia	68	2.35 (1.71,3.23) *	2.34 (29.48) *	0.81 (−0.87)	1.75 (1.28)
	Pain in extremity	66	2.00 (1.47,2.74) *	2.00 (19.86) *	0.68 (−1.00)	1.60 (1.17)
	Back pain	37	0.73 (0.51,1.05)	0.73 (2.95)	−0.35 (−2.03)	0.78 (0.55)
	Muscle spasms	30	2.02 (1.27,3.21) *	2.02 (9.24) *	0.69 (−1.01)	1.61 (1.01)
	Muscular weakness	24	1.19 (0.74,1.91)	1.19 (0.52)	0.18 (−1.51)	1.14 (0.71)
	Bone pain	20	1.64 (0.95,2.82)	1.63 (3.21)	0.50 (−1.21)	1.41 (0.82)
	Arthritis	14	2.12 (1.07,4.20) *	2.12 (4.86) *	0.73 (−1.01)	1.66 (0.84)
	Myositis	13	2.07 (1.02,4.20) *	2.07 (4.27) *	0.71 (−1.03)	1.63 (0.81)
	Musculoskeletal stiffness	12	2.79 (1.27,6.13) *	2.79 (7.18) *	0.95 (−0.81)	1.93 (0.88)
Limb discomfort	11	4.16 (1.67,10.35) *	4.16 (11.12) *	1.22 (−0.57)	2.33 (0.94)	
Respiratory, Thoracic and Mediastinal Disorders	Dysphonia	81	1.40 (1.08,1.83) *	1.40 (6.37)	0.35 (−1.33)	1.27 (0.98)
	Dyspnoea	44	0.44 (0.32,0.60)	0.44 (27.30)	−0.96 (−2.64)	0.51 (0.37)
	Cough	37	1.05 (0.72,1.52)	1.05 (0.06)	0.05 (−1.63)	1.03 (0.71)
	Pneumonitis	21	1.41 (0.84,2.37)	1.41 (1.72)	0.36 (−1.35)	1.28 (0.76)
	Pulmonary embolism	20	0.51 (0.32,0.82)	0.51 (7.96)	−0.78 (−2.46)	0.58 (0.36)
	Pleural effusion	14	0.78 (0.44,1.41)	0.78 (0.66)	−0.27 (−1.97)	0.83 (0.46)
Investigations	Blood pressure increased	148	1.17 (0.97,1.42)	1.17 (2.73)	0.17 (−1.50)	EBGM新增
	Weight decreased	110	1.60 (1.27,2.02) *	1.59 (16.01)	0.47 (−1.20)	1.12 (0.93)
	Platelet count decreased	51	0.48 (0.36,0.65)	0.49 (24.29)	−0.85 (−2.52)	1.39 (1.10)
	Blood pressure abnormal	43	7.68 (4.38,13.48) *	7.65 (70.56) *	1.53 (−0.18)	0.56 (0.41)
	Hepatic enzyme increased	28	2.12 (1.31,3.44) *	2.12 (9.73) *	0.73 (−0.97)	2.88 (1.64)
	Blood thyroid stimulating hormone increased	25	2.05 (1.23,3.40) *	2.04 (7.97) *	0.70 (−1.01)	1.66 (1.02)
	Thyroid function test abnormal	21	3.74 (1.97,7.10) *	3.74 (18.85) *	1.15 (−0.58)	1.62 (0.98)
	White blood cell count decreased	20	0.55 (0.34,0.88)	0.55 (6.26)	−0.69 (−2.38)	2.22 (1.17)
	Thyroid hormones increased	16	8.08 (3.16,20.65) *	8.07 (27.03) *	1.55 (−0.22)	0.62 (0.38)
	Aspartate aminotransferase increased	14	1.14 (0.62,2.12)	1.14 (0.19)	0.14 (−1.57)	2.93 (1.14)
	Blood magnesium decreased	14	1.25 (0.67,2.32)	1.25 (0.48)	0.23 (−1.48)	1.10 (0.60)
	Alanine aminotransferase increased	13	0.98 (0.53,1.84)	0.98 (0.00)	−0.02 (−1.73)	1.17 (0.63)
	Thyroid hormones decreased	13	4.37 (1.87,10.24) *	4.37 (13.82) *	1.25 (−0.52)	0.99 (0.53)
	Liver function test increased	12	3.03 (1.36,6.74) *	3.02 (8.14) *	1.01 (−0.75)	2.38 (1.02)
	Blood glucose increased	12	1.51 (0.76,3.03)	1.51 (1.39)	0.42 (−1.31)	2.01 (0.90)
	Blood creatinine increased	11	0.79 (0.41,1.54)	0.79 (0.48)	−0.26 (−1.97)	1.34 (0.67)
	Red blood cell count decreased	11	1.33 (0.65,2.71)	1.33 (0.63)	0.30 (−1.43)	0.84 (0.43)
	Liver function test abnormal	10	2.02 (0.91,4.49)	2.02 (3.08) *	0.69 (−1.07)	1.23 (0.60)
Reproductive System and Breast Disorders	Vaginal haemorrhage	16	0.83 (0.48,1.45)	0.83 (0.41)	−0.20 (−1.90)	0.87 (0.50)
Vascular disorders	Hypertension	182	0.76 (0.64,0.89)	0.76 (10.94)	−0.30 (−1.97)	0.81 (0.69)
	Hypotension	30	0.63 (0.43,0.94)	0.63 (5.25)	−0.52 (−2.20)	0.70 (0.47)
	Blood pressure fluctuation	20	1.41 (0.83,2.39)	1.41 (1.61)	0.35 (−1.35)	1.28 (0.75)
Blood and Lymphatic System Disorders	Thrombocytopenia	34	0.74 (0.51,1.08)	0.74 (2.51)	−0.34 (−2.02)	0.79 (0.54)
	Anaemia	28	0.43 (0.29,0.65)	0.44 (17.91)	−0.98 (−2.66)	0.51 (0.34)
	Neutropenia	11	0.39 (0.21,0.73)	0.39 (9.24)	−1.12 (−2.81)	0.46 (0.25)
	Lymphadenopathy	10	2.75 (1.17,6.48) *	2.75 (5.84) *	0.94 (−0.84)	1.92 (0.81)
Eye disorders	Visual impairment	277	1.37 (1.06,1.76) *	1.36 (5.75)	0.32 (−1.35)	1.25 (0.97)
Vision blurred						
Continued						

System Organ Class (SOC)	Preferred terms (PTs)	Cases (n)	ROR (95% two-sided CI)	PRR (χ2)	IC (IC025)	EBGM (EBGM05)
Cardiac disorders	Cardiac disorder	11	1.59 (0.76,3.29)	1.58 (1.56)	0.47 (-1.27)	1.38 (0.67)
	Myocarditis	10	0.44 (0.23,0.85)	0.44 (6.30)	-0.97 (-2.67)	0.51 (0.26)
Psychiatric disorders	Insomnia	23	1.02 (0.64,1.64)	1.02 (0.01)	0.02 (-1.67)	1.02 (0.63)
	Confusional state	16	0.60 (0.35,1.02)	0.60 (3.63)	-0.59 (-2.28)	0.66 (0.39)
	Anxiety	13	0.73 (0.40,1.33)	0.73 (1.07)	-0.36 (-2.06)	0.78 (0.43)

**Table 3.** Signal strength of AEs of immune checkpoint inhibitors at the preferred terms level in FAERS database. \*Indicates statistically significant signals in algorithm. ROR, reporting odds ratio; CI, confidence interval. PRR, proportional reporting ratio; χ2, chi-squared. IC, information component; IC025, the lower limit of the 95% CI of the IC. EBGM, empirical Bayesian geometric mean; EBGM05, the lower limit of 95% CI of EBGM.

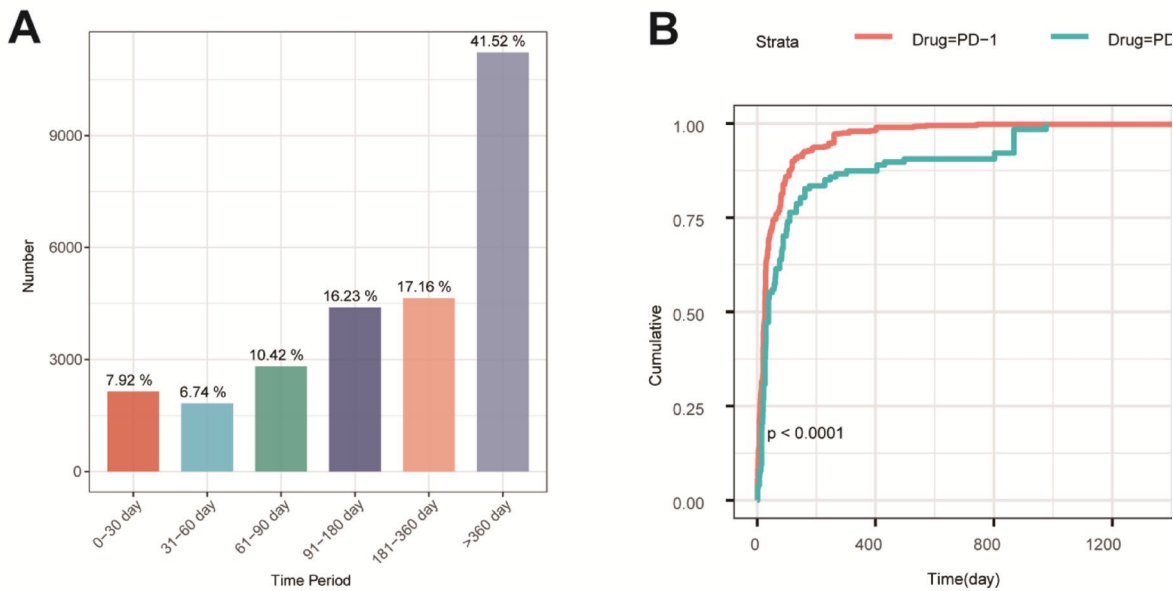


**Fig. 5.** Differences Between PD-1 and PD-L1 Immune Responses. (A)The number of onset times of ICIs-associated AEs at different time periods.(B) The significant difference in the cumulative incidence of ICIs AEs Between PD-1 and PD-L1 treatment.

Drugs	Cases (n)	TTO (days)	P	Weibull distribution		Failure type
				Scale parameter (95% two-sided CI)	Shape parameter (95% two-sided CI)	
PD-1	240	28 (12–79.25)	<0.0001	58.57 (47.46, 69.69)	0.71 (0.64, 0.77)	Early Failure
PD-L1	61	58 (22–132)		111.51 (71.00, 152.03)	0.73 (0.60, 0.87)	Early Failure

**Table 4.** Time-to-onset analysis for signals with PD-1/PD-L1.

Further analysis suggested that the accelerated immune response induced by PD-1 inhibitors may be closely linked to their impact on specific immune cell sub-clusters. Our pathway enrichment analysis revealed that CD8 + cytotoxic T cells and Tfh cells were enriched in several key signaling pathways. These included cytokine–cytokine receptor interaction, chemokine signaling, and viral protein interaction with cytokine and cytokine receptors pathways. Notably, these pathways are closely associated with CXCL signaling<sup>46,47</sup>. Through cell communication analysis, we observed that PD-1 inhibitors may promote interactions between CD8 + cytotoxic T cells and other immune cells in the tumor microenvironment. These interactions were mediated by specific ligand–receptor pairs, such as CXCL12–CXCR4 and CXCL16–CXCR6. Such communications may intensify the local immune response, both in magnitude and speed. For example, CXCR4 is a key receptor involved in immune cell migration and activation, especially in CD8 + T cells. Its high expression may allow these cells to rapidly respond to immune signals within the tumor microenvironment, thereby amplifying the immune response<sup>48</sup>. In contrast, Treg cells showed weaker signaling through this pathway, suggesting a less dominant role in maintaining immunosuppression. This differential signaling may explain the faster onset of irAEs observed

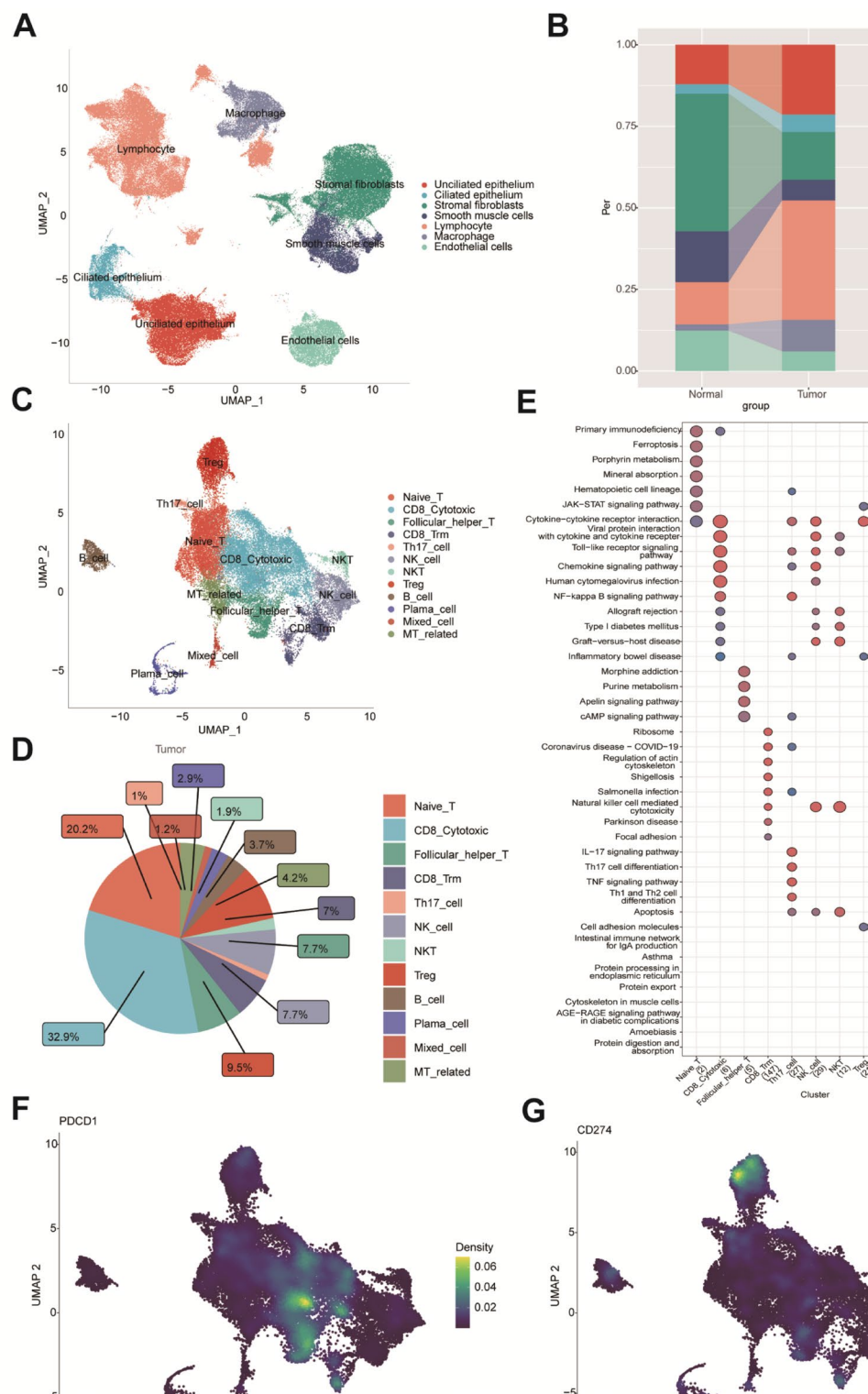


**Fig. 6.** Provided a comprehensive overview of human EC from Single-Cell Transcriptomics data. (A) Illustrated 7 cell clusters within the microenvironment using UMAP plots. (B) Illustrated the proportion of all cell types through bar plots. (C) Revealed lymphocytes divided into 12 sub-clusters. (D) Illustrated the proportion of lymphocyte sub-clusters through pie plots. (E) Showed enrichment pathways of the lymphocyte sub-clusters. (F) Displayed the expression of PDCD1 gene (PD-1) in lymphocyte sub-clusters. (G) Displayed the expression of CD274 gene (PD-L1) in lymphocyte sub-clusters.

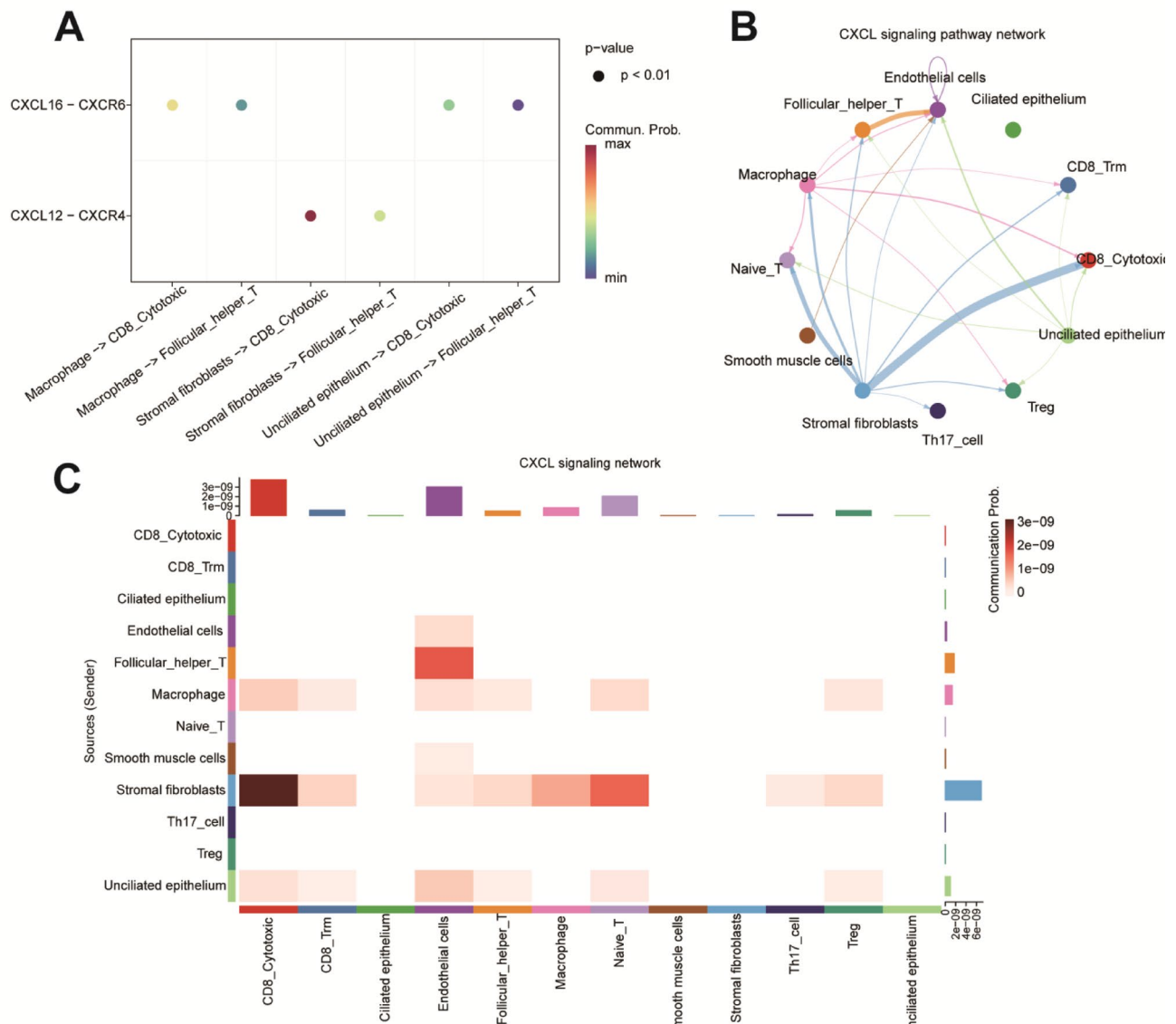


**Fig. 7.** Cell Communication in the Endometrial Microenvironment. **(A)** Receptor-ligand plots showed strong interactions between CD8 + cytotoxic T cells and Tfh cells with other cells mediated by CXCL12-CXCR4 and CXCL16-CXCR6. **(B)** NetVisual chord plots illustrated the strong communication between CD8 + cytotoxic T cells and Tfh cells with important cells through CXCL signaling pathway. **(C)** The heatmap displayed the strong communication between CD8 + cytotoxic T cells and Tfh cells with important cells through CXCL signaling pathway.

with PD-1 inhibitors compared to PD-L1 inhibitors. Previous studies have shown that blocking CXCR4 enhanced CD8 + T-cell mobilization and activation, especially when combined with PD-1 inhibitors. This highlighted the pivotal role of the CXCR4 axis in regulating T-cell trafficking and activation, which may contribute to enhanced immune responses and the rapid onset of irAEs<sup>49</sup>.

Moreover, the immune response triggered by PD-1 inhibitors was not limited to T cells alone. The high abundance of CD8 + cytotoxic T cells and Tfh cells, along with their strong interactions with other immune cells, may contribute to the rapid development of irAEs. Data from the FAERS database further support this observation, showing that many AEs are associated with CD8 + T cell-mediated responses, such as tissue damage and excessive inflammation. Based on this evidence, we hypothesized that CXCR6 expression may be involved in specific responses to PD-1 inhibitors, whereas CXCR4 may play a broader role in immune modulation and microenvironmental imbalance. Together, they may constitute a rapid mechanism underlying the occurrence of irAEs<sup>50</sup>.

From a methodological perspective, this study's strengths included the utilization of a large-scale dataset and scRNA-seq data. We aimed to enhance the reliability of the data analysis by rigorously cleaning and standardizing a substantial set of ICI-related reports from the FAERS database, with particular attention given to



duplicate reports and missing data to reduce potential biases. To improve the sensitivity of signal detection and accommodate variability among different algorithms, we applied four established disproportionality methods: PRR, ROR, BCPNN, and MGPS. These methods differ in statistical foundations—PRR and ROR are frequentist approaches using contingency tables, while BCPNN and MGPS are Bayesian models designed to handle data sparsity and estimate variability through prior distributions<sup>51,52</sup>. Since each algorithm has its own strengths and limitations, we combined multiple methods to broaden the scope of detection and validate the findings from diverse perspectives, aiming to produce more reliable signal detection outcomes<sup>51–53</sup>. To our knowledge, this was one of the few studies to systematically analyze large-scale adverse event data related to ICIs in EC, particularly within the FAERS database. Furthermore, single-cell transcriptomics analysis enabled a more detailed classification of immune cell sub-clusters and their interaction patterns, offering preliminary insights into the molecular mechanisms by which PD-1 inhibitors may contribute to ADRs from a cell communication perspective.

These findings may provide preliminary clues for the early identification and management of irAEs, indicating that, with further validation, clinicians could potentially improve risk assessment in patients receiving PD-1 inhibitors. This may inform future efforts toward personalized treatment strategies based on the patient's immune landscape. Moreover, the role of specific immune cell sub-clusters in irAEs warrants further investigation, which could eventually guide the development of targeted approaches to enhance the safety and efficacy of immune therapies.

However, despite providing new insights, this study had several limitations that should be acknowledged. First, as a spontaneous reporting system, FAERS is inherently prone to reporting bias, underreporting, and variability in data quality. The database may not capture all potential drug-related AEs, and the reported events are often skewed toward more severe or novel cases, which limits the generalizability of the findings. Consequently, these data cannot be used to estimate the actual incidence of AEs. Second, the lack of detailed clinical context in FAERS reports hindered the ability to establish a definitive causal relationship between ICIs and the reported AEs. Third, while scRNA-seq analysis provided insights into immune cell sub-clusters and their interactions, the findings were based on a limited sample size and may not fully represent the heterogeneity of immune responses across different patient populations. Finally, the study's conclusions were primarily hypothesis-generating, and further validation is required through prospective clinical studies, larger datasets, and mechanistic investigations using animal models or in vitro systems. Future research should also explore the integration of multi-omics data and longitudinal clinical follow-up to identify robust biomarkers of immune toxicity and refine predictive models for irAEs.

## Conclusion

This study integrated large-scale data analysis from the FAERS database with scRNA-seq data to explore potential mechanisms underlying irAEs in EC immunotherapy. Our findings suggested that PD-1 inhibitors may contribute to the development of rapid irAEs, potentially through compensatory activation of the CXCR4 and CXCR6 pathways. By identifying key receptor-ligand interactions, this study provided preliminary insights that could inform future efforts to optimize immunotherapy efficacy and manage immune toxicity. These results underscored the importance of pharmacovigilance in monitoring irAEs associated with ICIs and highlighted potential avenues for improving personalized treatment strategies. However, it is important to acknowledge the limitations of this study, including the inherent biases of the FAERS database, the exploratory nature of the scRNA-seq analysis, and the lack of direct clinical validation. Further research, including prospective clinical studies and mechanistic investigations, is needed to validate these findings and to deepen our understanding of the safety profile of ICIs in EC immunotherapy.

## Data availability

The data that support the findings of this study are openly available in FAERS database at <https://fis.fda.gov/extensions/FPD-QDE-FAERS/FPDQDE-FAERS.html>. The datasets generated and/or analysed during the current study have been deposited on SRA database (accession number PRJNA650549), NCBI SRA database under the accession number SRP349751, and the Gene Expression Omnibus (accession number GSE173682).

Received: 18 February 2025; Accepted: 15 May 2025

Published online: 28 May 2025

## References

1. Xia, C. et al. Cancer statistics in China and United States, 2022: profiles, trends, and determinants. *Chin. Med. J. (Engl)*. **135** (5), 584–590 (2022).
2. Miller, K. D. et al. Cancer treatment and survivorship statistics, 2022. *CA Cancer J. Clin.* **72** (5), 409–436 (2022).
3. Marín-Jiménez, J. A. et al. Facts and hopes in immunotherapy of endometrial cancer. *Clin. Cancer Res.* **28** (22), 4849–4860 (2022).
4. Pardoll, D. M. The blockade of immune checkpoints in cancer immunotherapy. *Nat. Rev. Cancer*. **12** (4), 252–264 (2012).
5. Eskander, R. N. et al. Pembrolizumab plus chemotherapy in advanced endometrial cancer. *N Engl. J. Med.* **388** (23), 2159–2170 (2023).
6. Gómez-Raposo, C. et al. Immune checkpoint inhibitors in endometrial cancer. *Crit. Rev. Oncol. Hematol.* **161**, 103306 (2021).
7. Mirza, M. R. et al. Dostarlimab for primary advanced or recurrent endometrial cancer. *N Engl. J. Med.* **388** (23), 2145–2158 (2023).
8. Marabelle, A. et al. Efficacy of pembrolizumab in patients with noncolorectal high microsatellite instability/mismatch repair-deficient cancer: results from the phase II KEYNOTE-158 study. *J. Clin. Oncol.* **38** (1), 1–10 (2020).
9. Brooks, R. A. et al. Current recommendations and recent progress in endometrial cancer. *CA Cancer J. Clin.* **69** (4), 258–279 (2019).
10. Gómez-Banoy, N. et al. Body mass index and adiposity influence responses to immune checkpoint inhibition in endometrial cancer. *J. Clin. Invest.* **134** (17), e180516 (2024).

11. Huang, D. et al. Efficacy and safety of immune checkpoint inhibitors for advanced or recurrent endometrial cancer: a systematic review and network meta-analysis. *BMC Cancer*. **24** (1), 1298 (2024).
12. Li, H. et al. Thromboembolic events associated with immune checkpoint inhibitors: A real-world study of data from the food and drug administration adverse event reporting system (FAERS) database. *Int. Immunopharmacol.* **98**, 107818 (2021).
13. Zhou, C. et al. Psychiatric disorders associated with immune checkpoint inhibitors: a pharmacovigilance analysis of the FDA adverse event reporting system (FAERS) database. *EclinicalMedicine* **59**, 101967 (2023).
14. Raschi, E. et al. The value of case reports and spontaneous reporting systems for pharmacovigilance and clinical practice. *Br. J. Dermatol.* **184** (3), 581–583 (2021).
15. Bihan, K. et al. Uses of pharmacovigilance databases: an overview. *Therapie* **75** (6), 591–598 (2020).
16. Liu, Z. et al. A single-cell atlas reveals immune heterogeneity in anti-PD-1-treated non-small cell lung cancer. *Cell* S0092-8674(25)00291-0 (2025).
17. Ren, X. et al. Single-cell transcriptomic analysis highlights origin and pathological process of human endometrioid endometrial carcinoma. *Nat. Commun.* **13** (1), 6300 (2022).
18. Zhang, Y. et al. Single-cell analyses reveal key immune cell subsets associated with response to PD-L1 Blockade in triple-negative breast cancer. *Cancer Cell*. **39** (12), 1578–1593e8 (2021).
19. Ren, X. et al. Immune-related adverse events of immune checkpoint inhibitors combined with angiogenesis inhibitors: A real-world pharmacovigilance analysis of the FDA adverse event reporting system (FAERS) database (2014–2022). *Int. Immunopharmacol.* **136**, 112301 (2024).
20. Zhai, Y. et al. Endocrine toxicity of immune checkpoint inhibitors: a real-world study leveraging US food and drug administration adverse events reporting system. *J. Immunother Cancer*. **7** (1), 286 (2019).
21. Sarntivijai, S. et al. Linking MedDRA(®)-Coded clinical phenotypes to biological mechanisms by the ontology of adverse events: A pilot study on tyrosine kinase inhibitors. *Drug Saf.* **39** (7), 697–707 (2016).
22. Chen, C. et al. Immune-related adverse events associated with immune checkpoint inhibitors: an updated comprehensive disproportionality analysis of the FDA adverse event reporting system. *Int. Immunopharmacol.* **95**, 107498 (2021).
23. Yang, Y. et al. Delayed immune-related adverse events profile associated with immune checkpoint inhibitors: a real-world analysis. *Front. Pharmacol.* **15**, 1453429 (2024).
24. Hauben, M. & Reich, L. Safety related drug-labelling changes: findings from two data mining algorithms. *Drug Saf.* **27** (10), 735–744 (2004).
25. Rothman, K. J., Lanes, S. & Sacks, S. T. The reporting odds ratio and its advantages over the proportional reporting ratio. *Pharmacoepidemiol Drug Saf.* **13** (8), 519–523 (2004).
26. van Puijtenbroek, E. P. et al. A comparison of measures of disproportionality for signal detection in spontaneous reporting systems for adverse drug reactions. *Pharmacoepidemiol Drug Saf.* **11** (1), 3–10 (2002).
27. Almenoff, J. S. et al. Novel statistical tools for monitoring the safety of marketed drugs. *Clin. Pharmacol. Ther.* **82** (2), 157–166 (2007).
28. Guo, Y. et al. Phenotyping of immune and endometrial epithelial cells in endometrial carcinomas revealed by single-cell RNA sequencing. *Aging (Albany NY)*. **13** (5), 6565–6591 (2021).
29. Regner, M. J. et al. A multi-omic single-cell landscape of human gynecologic malignancies. *Mol. Cell*. **81** (23), 4924–4941e10 (2021).
30. Sun, S. et al. Accuracy, robustness and scalability of dimensionality reduction methods for single-cell RNA-seq analysis. *Genome Biol.* **20** (1), 269 (2019).
31. Becht, E. et al. Dimensionality reduction for visualizing single-cell data using UMAP. *Nat. Biotechnol.* **37** (1), 38–44 (2019).
32. Jin, S. et al. Inference and analysis of cell-cell communication using cellchat. *Nat. Commun.* **12** (1), 1088 (2021).
33. Yu, G. et al. ClusterProfiler: an R package for comparing biological themes among gene clusters. *OMICS* **16** (5), 284–287 (2012).
34. Ogata, H. et al. Kyoto encyclopedia of genes and genomes. *Nucleic Acids Res.* **27** (1), 29–34 (1999).
35. Alsaab, H. O. et al. PD-1 and PD-L1 checkpoint signaling Inhibition for Cancer immunotherapy: mechanism, combinations, and clinical outcome. *Front. Pharmacol.* **8**, 561 (2017).
36. Gong, J. et al. Development of PD-1 and PD-L1 inhibitors as a form of cancer immunotherapy: a comprehensive review of registration trials and future considerations. *J. Immunother Cancer*. **6** (1), 8 (2018).
37. Chang, C. et al. Immune checkpoint inhibitors and Immune-Related adverse events in patients with advanced melanoma: A systematic review and network Meta-analysis. *JAMA Netw. Open*. **3** (3), e201611 (2020).
38. Wang, Y. et al. Treatment-Related adverse events of PD-1 and PD-L1 inhibitors in clinical trials: A systematic review and Meta-analysis. *JAMA Oncol.* **5** (7), 1008–1019 (2019).
39. Pillai, R. N. et al. Comparison of the toxicity profile of PD-1 versus PD-L1 inhibitors in non-small cell lung cancer: A systematic analysis of the literature. *Cancer* **124** (2), 271–277 (2018).
40. Puzanov, I. et al. Managing toxicities associated with immune checkpoint inhibitors: consensus recommendations from the society for immunotherapy of Cancer (SITC) toxicity management working group. *J. Immunother Cancer*. **5** (1), 95 (2017).
41. Verzoni, E. et al. Real-world efficacy and safety of nivolumab in previously-treated metastatic renal cell carcinoma, and association between immune-related adverse events and survival: the Italian expanded access program. *J. Immunother Cancer*. **7** (1), 99 (2019).
42. Postow, M. A., Sidlow, R. & Hellmann, M. D. Immune-Related adverse events associated with immune checkpoint Blockade. *N Engl. J. Med.* **378** (2), 158–168 (2018).
43. Zhou, X. et al. Are immune-related adverse events associated with the efficacy of immune checkpoint inhibitors in patients with cancer? A systematic review and meta-analysis. *BMC Med.* **18** (1), 87 (2020).
44. Khoja, L. et al. Tumour- and class-specific patterns of immune-related adverse events of immune checkpoint inhibitors: a systematic review. *Ann. Oncol.* **28** (10), 2377–2385 (2017).
45. Tumeh, P. C. et al. PD-1 Blockade induces responses by inhibiting adaptive immune resistance. *Nature* **515** (7528), 568–571 (2014).
46. Zlotnik, A. & Yoshie, O. The chemokine superfamily revisited. *Immunity* **36** (5), 705–716 (2012).
47. Bule, P. et al. Chemokine-Directed tumor microenvironment modulation in Cancer immunotherapy. *Int. J. Mol. Sci.* **22** (18), 9804 (2021).
48. Harper, M. M. et al. Interaction of immune checkpoint PD-1 and chemokine receptor 4 (CXCR4) promotes a malignant phenotype in pancreatic cancer cells. *PLoS One*. **17** (7), e0270832 (2022).
49. Seo, Y. D. et al. Mobilization of CD8(+) T cells via CXCR4 Blockade facilitates PD-1 checkpoint therapy in human pancreatic Cancer. *Clin. Cancer Res.* **25** (13), 3934–3945 (2019).
50. Wang, B. et al. CXCR6 is required for antitumor efficacy of intratumoral CD8(+) T cell. *J. Immunother. Cancer* **9**(8), e003100 (2021).
51. Wu, X. et al. Post-Marketing safety concerns with Upadacitinib: A disproportionality analysis of the FDA adverse event reporting system. *Expert Opin. Drug Saf.* **22** (10), 975–984 (2023).
52. Lin, J. et al. Safety of Tildrakizumab: a disproportionality analysis based on the FDA adverse event reporting system (FAERS) database from 2018–2023. *Front. Pharmacol.* **15**, 1420478 (2024).
53. Song, Y. et al. A real-world pharmacovigilance study of Omalizumab using disproportionality analysis in the FDA adverse drug events reporting system database. *Sci. Rep.* **15** (1), 8045 (2025).

## Acknowledgements

This work was supported by the National Natural Science Foundation of China (No. 82271678), the Natural Science Foundation of Fujian Province (No. 2022 J02058 and No. 2023 J01623).

## Author contributions

The study was conceived, designed by Qionghua Chen and Jianfa Lan. Lu Zhang and Mengjie Yang performed bioinformatics analysis of data and participated in writing the manuscript. Yiqian Zhang helped with bioinformatics analysis. All authors read and approved the final manuscript.

## Declarations

## Competing interests

The authors declare no competing interests.

## Ethical approval

This study utilized publicly available, de-identified FAERS data, and therefore did not require approval from an ethics committee or informed consent.

## Additional information

**Supplementary Information** The online version contains supplementary material available at <https://doi.org/10.1038/s41598-025-02723-3>.

**Correspondence** and requests for materials should be addressed to J.L. or Q.C.

**Reprints and permissions information** is available at [www.nature.com/reprints](http://www.nature.com/reprints).

**Publisher's note** Springer Nature remains neutral with regard to jurisdictional claims in published maps and institutional affiliations.

**Open Access** This article is licensed under a Creative Commons Attribution-NonCommercial-NoDerivatives 4.0 International License, which permits any non-commercial use, sharing, distribution and reproduction in any medium or format, as long as you give appropriate credit to the original author(s) and the source, provide a link to the Creative Commons licence, and indicate if you modified the licensed material. You do not have permission under this licence to share adapted material derived from this article or parts of it. The images or other third party material in this article are included in the article's Creative Commons licence, unless indicated otherwise in a credit line to the material. If material is not included in the article's Creative Commons licence and your intended use is not permitted by statutory regulation or exceeds the permitted use, you will need to obtain permission directly from the copyright holder. To view a copy of this licence, visit <http://creativecommons.org/licenses/by-nc-nd/4.0/>.

© The Author(s) 2025